VOL. 20, NO. 1, JANUARY 2025 ISSN 1819-6608
ARPN Journal of Engineering and Applied Sciences

www.arpnjournals.com

OPTIMAL PREDICTION OF AL-8112 ALLOY CUTTING FORCE VIA MACHINING USING ANFIS-PSO AND ANFIS-GA FOR A SUSTAINABLE CUTTING PROCESS

Imhade P. Okokpujie[1,2]
[1]Department of Mechanical and Industrial Engineering Technology, University of Johannesburg, Johannesburg, South Africa
[2]Department of Mechanical and Mechatronics Engineering, Afe Babalola University, Ado Ekiti, Nigeria
E-Mail: ip.okokpujie@abuad.edu.ng

ABSTRACT

Cutting force prediction is one of the important responses that is highly considered during the manufacturing process, mostly via computer numerical control machine. Parameters employed in the industry to transform raw materials into finished products, such as the machining parameters, have many challenges during operations. This can lead to high cutting force, which leads to high energy consumption during operations. Therefore, this study focuses on the optimal prediction of the cutting force of aluminium 8112 alloys via machining using ANFIS-PSO and ANFIS-GA for a sustainable cutting process. The experimental data was obtained from a machining experiment with five cutting parameters: cutting speed, helix angle, feed rate, machining length, and depth at five levels. Also, this experiment was carried out in an eco-friendly machining lubricant (TiO_2 nano-lubricant), and a dynamometer was used to record the cutting force during operations for every one of the 50 runs of the experiment. The ANFIS-PSO and ANFIS-GA were employed to predict the cutting force with a ratio of training and testing of 35:15. The results show that ANFIS-PSO and the ANFIS-GA predicted the cutting force with 91.98% and 93.98% for the training data of the model and 90.11% and 92.1% for the testing data respectively. The interaction between the five cutting parameters shows that the helix angle and the machining length have a good relationship during the machining process. Also, the results show that the cutting force decreases as the helix angle decreases with the machining length.

Keywords: cutting force; Al8012 alloy; machining; ANFIS-PSO; TiO_2 nano-lubricant

Manuscript Received 6 November 2024; Revised 7 January 2025; Published 10 February 2025

1. INTRODUCTION

Cutting force is a crucial sign of the energy and power required for machining. Reducing the frictional forces at the rake face and flank face will help to reduce the machining forces [1]. Both cutting force and friction can be reduced by choosing the proper cutting fluid. Axial and radial forces are the two main types of cutting forces. The direction of action of axial forces is parallel to the spindle. Perpendicular to the spindle, radial forces operate [2]. The part material and the tool's substrate, coating, rake angle, and helix angle all affect the specific cutting force coefficients. No universal guidelines can be applied to forecast the values of the coefficients because the link between them and these parameters is so intricate. The precise and extremely dynamic force measurements made possible by this structure enable prompt quantification of even the tiniest changes in the process chain. Cutting forces Fc, feed forces Ff, and passive forces Fp can all be quantified in terms of three components using multi-component dynamometers. Therefore, the study of the machining of aluminium alloy is very significant in the manufacturing industry for its application in mechanical, design, and production processes. Al8012 Alloy is an 8000 series aluminium with an excellent strength-to-weight ratio. However, optimal prediction is highly needed for material adhesion during machining. Aluminium alloys will be reduced since surface finishing and reduced cutting forces are needed to reduce the high energy consumption level during machining. Sustainable cutting fluid is also useful in reducing the cutting force because reducing the cutting force will reduce energy consumption during the application [3].

The lubricating oil wear, friction, heat, substance, and physical properties are all impacted by the presence of nanoparticles in it. One lubricant additive that shows promise for improving machining efficiency is titanium dioxide (TiO_2). Okokpujie et al. [4] study compared the effects of MWCNTs nano-lubricant and environmentally friendly vegetable oil-based TiO_2 on cutting force when machining AL-8112 alloys. Before being applied in machining using an ultrasonic vibrator and a magnetic stirrer, nanoparticles were introduced to the base oil as part of the lowest quantity lubrication process. The experiment used quadratic central composite designs to utilise five factors at five levels and fifty experimental runs. Helix angle (HA), spindle speed (SS), feed rate (FR), axial depth of cut (ADOC), and length of cut (LOC) are the input parameters. The outcomes demonstrate that applying the nanoparticle improves the vegetable oil's cutting force performance. When compared to MWCNTs, TiO_2 nano-lubricant lowers the cutting force by 0.26%, and when compared to vegetable oil, it decreases it by 6%. In addition, 5% less cutting force is required when using the MWCNT nano-lubricant than in a vegetable oil lubrication environment. This study shows that TiO_2 nano-vegetable lubricant is exceptional for machining operations. Besides the cutting fluid that reduces the cutting force during machining, there is a need for

prediction and optimisation tools for accuracy analysis for future works.

Genetic algorithm (GA) and particle swarm optimisation (PSO) are optimisation techniques for assessing the arbitrarily generated significant population for fitness functions. All of them use Homogenous Population Subgrouping to enhance the quality of the solution as the already fast process of clustering of the solution is further slowed down. GA is a presentation that develops a method by which it is possible to solve both restricted and unrestricted optimisation problems of a biological process that takes place in nature. The model revises a set of possible solutions to a problem regularly. GA randomly selects individuals of the current generation to be parents throughout every phase of the subsequent generation's progeny. The population mutates toward the best solution into the generations of the future. PSO, on the other hand, can be defined as a computing concept where the optimisation of algorithms, as well as other patterns characteristic of engineering and mathematics, is employed to solve problems, which, in the process, strives to optimise a candidate solution (particle)—relating to the firm or enterprise in matters of quality in some rated scale. It solves the problem by initiating a beginning population potential solutions while referring to them as particles and shifting their places in the search domain in a manner related to the position and velocity determinable by way of the basic formula, then shored by their respective occupational roles. PSO particles auto-update instead of crossover and mutation genetics, and candidates use their internal selection velocity.

In this work, Jain and Raj [5] aim to create a model to forecast the cutting forces involved in a turning operation. This work focuses on developing an adaptive neuro-fuzzy inference system (ANFIS) monitoring system that can identify cutting force based on cutting parameters such as spindle speed, feed, and depth of cut. One of the crucial characteristics that must be monitored and managed during the cutting processes to ascertain the workpiece's surface roughness and tool life is the cutting force. The main presumption was that as the tool wears, the cutting forces rise. Thus, the cutting force signal is expressed using the ANFIS model. The cutting force is predicted in this work using ANFIS. This modelling yielded a correlation coefficient (R) of 0.9976 and an average percentage error of 2.59%. The experimental data and the projected cutting force values obtained by ANFIS were compared. The comparison shows that the accuracy achieved by the ANFIS was quite good. This modelling yielded a correlation coefficient (R) of 0.9976 and an average percentage error of 2.59%. The ANFIS's prediction accuracy was as high as 97%. However, this article is limited because the study considered only three cutting parameters, which cannot justify the accuracy of the prediction. In the study of Okokpujie and Tartibu [6], a quadratic rotatable central composite design (QRCCD) was employed to predict the cutting force. The (QRCCD) predicted the cutting force with 89.70%, which in the standard prediction analysis is viable for forecasting the cutting force.

Therefore, this study aimed to conduct optimal prediction of the cutting force of Al8112 alloy via machining using an ANFIS-PSO and ANFIS-GA for a sustainable cutting process. The research considered five machining factors: cutting speed, feed rate, helix angle and length, and machining depth. The significance of this study is the implementation of ANFIS-PSO and ANFIS-GA in the prediction of Al8112 alloys, which has not been done before.

2. METHODOLOGY

The materials employed in this study are Al8112 alloys, TiO_2 nano lubricants, and high-speed steel, which are used as the cutting tool. The method used in the generation of the data and the artificial intelligence tool employed for the optimal prediction are discussed in the subsections.

2.1 Dataset Description for the Cutting Force

This experiment used the SIEG 3/10/0016 CNC machine to end-mill the AL8112 alloy. The CNC milling machine comprises three (3) x, y, and z planes. The end-milling process comprises five variables (spindle speed, feed rate, length of cut, depth of cut, and helix angle) and five levels of the experiment. The cutting fluid is a nano-lubricant composed of copra oil and titanium dioxide (TiO_2). There are multiple steps in this section. The following methods were employed in the experimental inquiry:

i. The rectangular plate made of aluminium 8112 alloys was cut into multiple machining lengths, namely 20, 30, 40, 50, and 60 mm. For TiO_2, 50 pieces were considered in a cut-off machine setting.
ii. TiO_2 nano-lubricants are ready for end-milling machining while the top of the CNC milling device is cleaned. Using various level cutting speeds of 2000, 2500, 3000, 3500, and 4000 (rpm), feed rates of 100, 150, 200, 250, and 300 (mm/min), machining depths from 1 to 3 (mm), and helix angle of 0 to 60 ºC.
iii. The end-milling tip's spindle head was fitted with a 13 mm-diameter High-Speed Steel (HSS) cutting tool.
iv. Securing the dynamometer and AL-8112 alloy with a vibration-reducing device after mounting them on the machine's bench bed.
v. When creating the CNC part software design, which contained specific commands for implementing different machining lengths, feed rates, machining, helix angles, and cutting speeds, the Y- and Z-axes were used as references.
vi. The dynamometer records the cutting force for each sample for 50 samples while the machining process is underway, using different machining parameters, as seen in Figure 1.

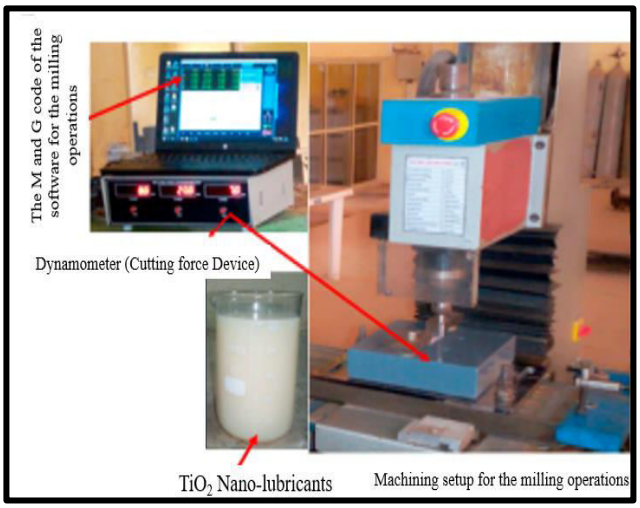

Figure-1. The experimental setup for the machining process.

During the machining experiment, the dynamometer measures the cutting force for each 50 samples in the three cutting conditions. As seen in Figure 1, with a strain gauge section, 350 OHMS span resistance, an ultimate voltage of 5 volts, and an indication range of 0–300 KGF, the dynamometer has four arms. The dynamometer contains three (3) stages that show the cutting forces along the X, Y, and Z axes for each machining process. Eq. (1) calculated the total cutting force following the measurement [15]. For this study, the directional cutting forces are C_x (X-axis), C_y (Y-axis), and C_z (Z-axis), and the resulting force is

$$C_f = \sqrt{C_x^2 + C_y^2 + C_z^2} \quad (1)$$

2.2 Method of the Prediction Process for the Cutting Force Prediction via ANFIS-PSO and ANFIS-GA

Segmentation jobs, rule-based procedure controls, recognising patterns issues, and approximate function issues are among the applications of ANFIS [7]. The best way to distribute membership functions is determined by the mapping relation between the input and output data in the ANFIS architecture, which combines fuzzy logic and artificial neural networks. Fuzzy logic (FL) theory and adaptive neural network (ANN) concepts are integrated in adaptive network frameworks. The fuzzy interference system (FIS) application was created using FL theory, and by trial and error, the membership functions (MF) of FIS were enhanced. The FIS model is built using the ANN process in the ANFIS approach. This makes it possible for the supplied data to train the neural network. Concurrently mapping the results are the factors in the Sugeno category IF-THEN rule structure.

Figure 2 depicts the overall layout of the ANFIS framework. This inference system consists of five different layers. This includes the following layers: the de-fuzzy layer (iv), the fuzzy layer (i), the product layer (ii), the normalised layer (iii), and the overall output layer (v). Each stratum has unique nodes represented by squares, adaptive nodes and changeable factors. Circles, on the other hand, represent the fixed nodes, where the factors never change. You can find the mathematical expression in Okokpujie and Tartibu [8]. The study takes into account two fuzzy if-then rules to describe the rules associated with each layer given in Eq.s (2) and (3):

$$Rule_1: if\ x\ is\ A_1\ and\ y\ is\ B_1\ then\ f = P_1x + q_1y + r_1 \quad (2)$$

$$Rule_2: if\ x\ is\ A_2\ and\ y\ is\ B_2\ then\ f = P_2x + q_2y + r_2 \quad (3)$$

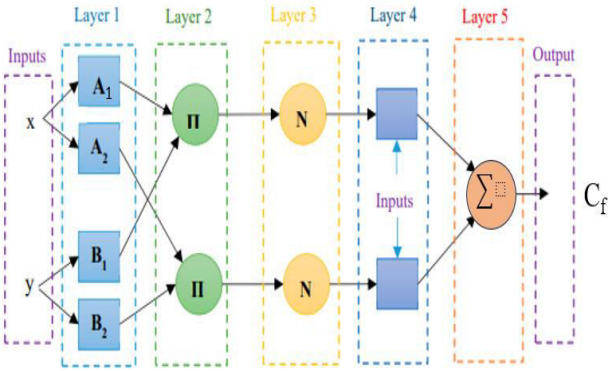

Figure-2. ANFIS architecture adopted for the cutting-force prediction analysis

If f is the output (linguistic variables), A_1 and B_1 are fuzzy sets, and x and y are the input variables. The following parameters—{pi}, {qi}, and {ri}—should be measured as part of the ANFIS training procedure. The following metrics can be used to gauge each layer's function:

First Layer: Every node (i) in this layer is defined by a membership function. Membership functions in fuzzy logic are used to make the variables fuzzy. These membership functions are curves that specify the mapping from a point in the input space to a membership value in the [0,1] interval. There are several membership functions, the most popular being the Gaussian, Trapzoidum, and Triangular types, which give Eq. (4) and Eq. (5) [9].

$$Q_{1.i} = \sigma_{A1(x)} \quad (4)$$

$$Q_{1.i} = \sigma_{B1(x)} \quad (5)$$

Where x is identified as Q_1 and node input, i is the membership function of A_i, which the Gaussian function often defines as follows in Eq. (6):

$$\sigma_{A1(x)} = \exp\frac{-(x-c)^2}{\sigma^2} \quad (6)$$

The antecedent parameters in this formula are the standard deviation (σ) and the centre of the Gaussian membership function (C), respectively. These parameters are important for membership functions, and the optimisation algorithm determines their worth.

Second Layer: The following relation determines a rule's firing strength is given in Eq. (7):

$$w_i = \sigma_{Ai(x)} \, X \, \sigma_{Bi(x)} \qquad i = 1.2 \qquad (7)$$

Third Layer: By dividing the projectile strength of the ith rule by the overall firing power of all rules, the firing strength of each rule is normalised in Eq. (8).

$$Q_{3.i} = \overline{w_i} = \frac{w_i}{w_1 + w_2} \quad i = 1.2 \qquad (8)$$

Fourth Layer: The fuzzy rule's outcome portion is measured in the manner described in Eq. (9):

$$Q_{4.i} = \overline{w_i} f_i = \overline{w_i}(p_i x + q_1 y + r_1) \qquad i = 1.2 \quad (9)$$

Where $\{p_i, q_i, r_i\}$ are the set of consequent parameters computed by the optimisation algorithm.

Fifty Layer: In this layer, all the outputs of the fourth layer are added to form Eq. (10).

$$Q_{5.i} = \sum_{i=1}^{R} \overline{w_i} f_i \qquad i = 1.2 \quad (10)$$

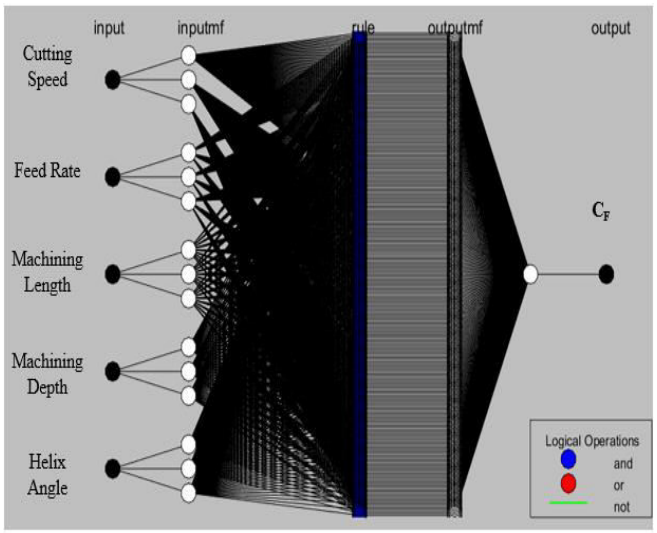

Figure-3. Neural network model for cutting force.

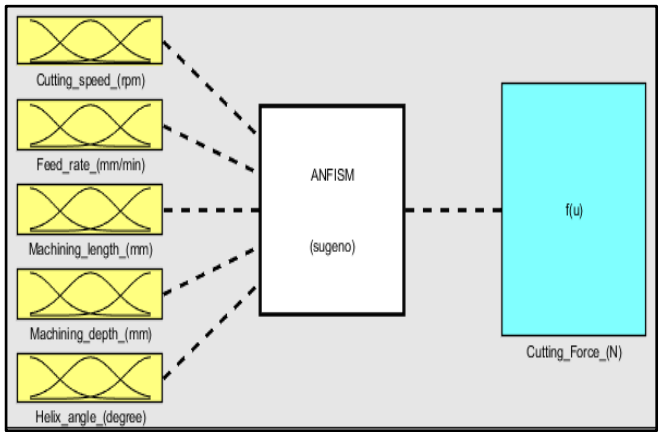

Figure-4. ANFIS structure.

Antecedent and consequent parameters are typically the two structural parameters of the ANFIS model [10]. The ANFIS model's antecedent and consequent parameters are typically changed using gradient-based techniques [11]. The fact that the solution is located in local optimality and that the gradient-based approaches' rate of convergence is slow is one of their problems [12]. Figs. 3 and 4 show the neural network model and ANFIS structure for cutting force. The problems with gradient-based approaches can be effectively resolved by applying metaheuristic algorithms using particle swarm optimisation (PSO) [13]. Figure 5 shows the method for the ANFIS-PSO, and Figure 6 the ANFIS-GA for the model using metaheuristic optimisation approaches PSO and GA.

One of the nature-inspired optimisation techniques is the PSO algorithm, which Hub and Kennedy originally developed in 1995 [14]. This approach mostly addresses large-scale numerical optimisation problems without knowledge of the target function gradient [15]. A population of potential solutions is randomly moved into the problem domain using a straightforward formula to solve a problem. Next, it investigates to locate the best possible global solution (each potential solution is referred to as a particle). Like the PSO algorithm, the method generates a population of randomly generated solutions by searching inside the problem area, akin to the genetic algorithm [16]. The hybrid ANN-GA model was trained using experimental data, and parametric analysis was carried out by altering the subsequent variables: Number of inhabitants: 25, 50, 75, and 100; five to ten hidden neurones are present, regarding the following the construction of the set to optimise the ANFIS using the GA algorithm, the chromosome encoding, fitness function, selection, recombination, and the scheme of evolution for the cutting force.

However, in contrast to genetic algorithms, the PSO method assigns a random velocity to every possible solution to the optimisation problem, that is, to every particle so that every iteration moves a single particle about its velocity. Furthermore, each particle in the PSO algorithm should store the optimal solution to the optimisation problem from the beginning of the program until the end of the last iteration, in contrast to the genetic algorithm. Like the evolutionary algorithm, the PSO algorithm is suitable for resolving continuous unconstrained maximisation problems. However, minor modifications to the function specification can also be applied to continuous state optimisation problems (such as minimisation or maximisation) [17]. These Particles all have five characteristics. The position is determined by the objective function corresponding to the current location, speed, optimal position, and quantity of objective function corresponding to the optimal position attained. Eqs determine each particle's position and speed inside the algorithm. (11) and (12). and according to the data from the preceding phase. These Eqs. designate r_1 and r_2 as random integers and c_1 and c_2 as the velocity constants. P-best, the weight of inertia comprises x, v, P^t, and G^t.

$$V_{ij}^{t}=\chi\left[\omega v_{ij}^{t-1}+c_1 r_1\left(p_{ij}^{t-1}-x_{ij}^{t-1}\right)+c_2 r_2\left(G_j^{t-1}-x_{ij}^{t-1}\right)\right] \quad (11)$$

$$x_{ij}^{t}=x_{ij}^{t-1}+v_{ij}^{t} \quad (12)$$

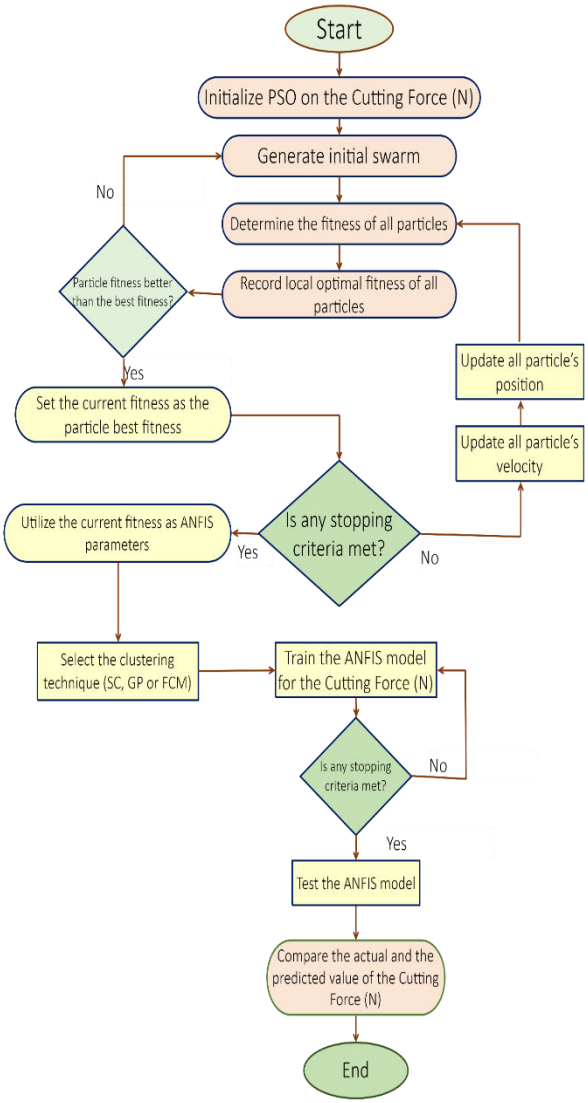

Figure-5. The procedure of the ANFIS-PSO prediction analysis.

The genetic algorithm model starts with a group of solutions, chromosomes. A new population is created by completing a previous population. The fitness of the new solution formed from selected offspring is signed. This process is carried out repeatedly until a condition, i.e., the optimal solution's improvement, is met. To accomplish this, the ANFS algorithm, part of the fitness function, plays an essential role in f(x). The fitness with the ANFIS algorithm function intervention is represented by equations (13) and (14)

$$f_1(x)-\frac{1}{m}\sqrt{\sum_{i}^{m} o(d_i-a_i)^2} \quad (13)$$

Where m is the number of characteristics, ai is the output derived from the ANFIS, and di is the predicted traffic volume. The next fitness function is given in Equation (15)

$$f_2(x)-\frac{1}{n-m}\sqrt{\sum_{i}^{m} m(d_i-a_i)^2} \quad (14)$$

$$f(x)-\frac{f_1(x)+f_2(x)}{2} \quad (15)$$

Where n is the overall number of input characteristics, di is the minimum, ai is the actual value of the traffic volume, and n -m indicates the leftover undesired attributes.

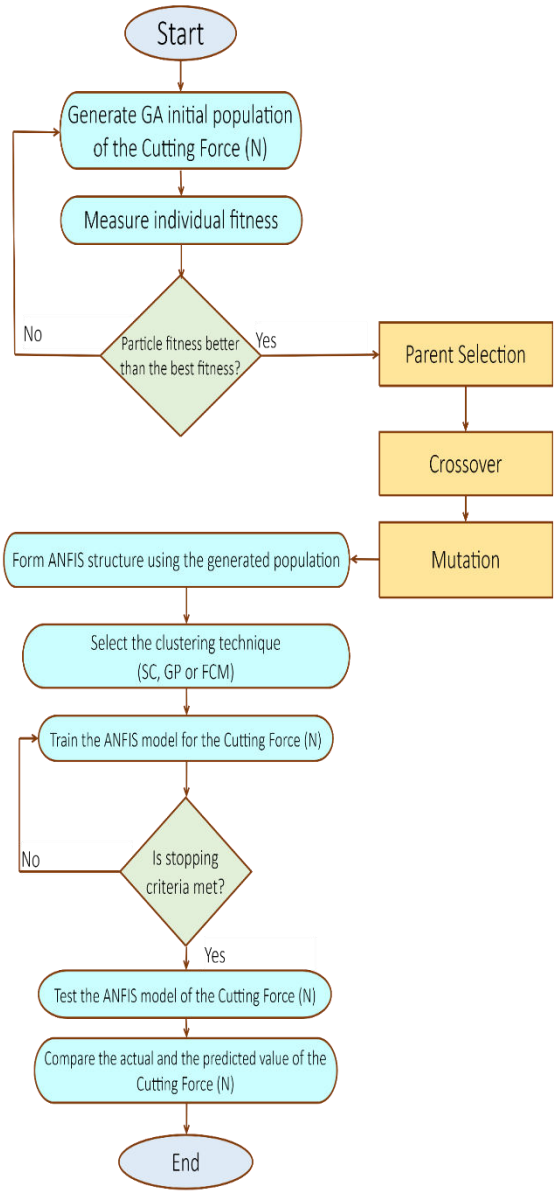

Figure-6. The procedure of the ANFIS-GA prediction analysis.

3. RESULTS AND DISCUSSIONS

The analysis of the results obtained from the prediction of the ANFIS-PSO and ANFIS-GA model for the training and testing data gives an overview of how the ANFIS-PSO and ANFIS-GA could predict the cutting force accurately.

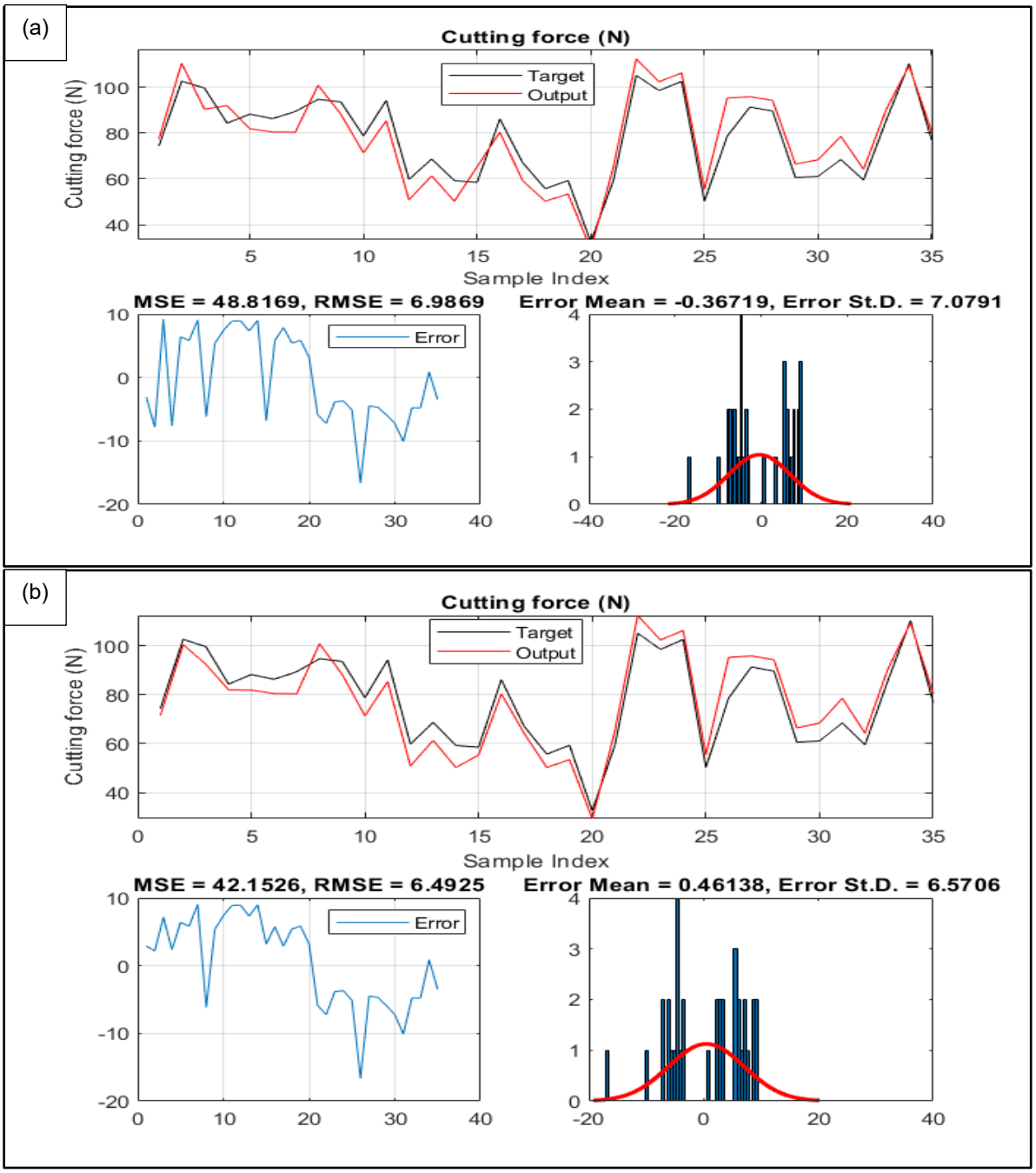

Figure-7. The comparative analysis of the Training data prediction with the experimental data for the (a) ANFIS-PSO and (b) the ANFIS-GA.

Table 1: Cutting force ANFIS-PSO and ANFIS GA performance metrics.

Performance metrics		ANFIS-PSO Training	ANFIS GA Training	ANFIS-PSO Testing	ANFIS GA Testing
Mean absolute percentage error	MAPE	8.7607	5.9482	9.8050	7.9694
Mean Absolute Error	MAE	6.4491	3.5283	5.8444	5.8277
mean absolute deviation	MAD	6.4176	2.6070	4.2541	5.7618
Root Mean Square Error	RMSE	6.9869	3.7641	6.1992	6.4925
Coefficient of Determination	R^2	0.919	0.9398	0.9011	0.921

Five machining parameters were considered for the study: cutting speed, feed rate, machining length, helix angle, and machining depth. Having a Coefficient of Determination R^2 of 0.9198 and 0.9398 for the training process for both the ANFIS-PSO and ANFIS-GA shows that the ANFIS-GA was able to perform excellently well in the prediction of the cutting force during the training session. For the testing process, the ANFIS-PSO has an R^2 value of 0.9011 and the ANFIS-GA R^2 value of 0.921 for the testing data. The RMSE of 6.9869 and 3.7641 for the training data and 6.1992 and 6.4925 for the testing prediction data were obtained for both ANFIS-PSO and ANFIS-GA. From the analysis via the ANFIS-PSO, the MAPE obtained are 8.7607 and 9.8050 for training and testing, respectively. Table 1 shows the ANFIS-PSO and ANFIS-GA performance metrics that justify the prediction accuracy. The data of 50 samples, 35 runs were used for the training process, and 15 runs were employed for the testing process.

Following the execution of ANFIS-PSO and ANFIS GA, Figure 7a and Figure 7b display the Train Data values for the ANFIS-PSO and the ANFIS GA, respectively. Plots of the target and output values were compared. This illustration also includes the calculated error values for Train Data. The ANFIS-PSO shows an MSE of 48.8169, RMSE of 6.9869, and a standard deviation of 7.091, while ANFIS-GA has an MSE of 42.1526, RMSE OF 6.4925, and standard deviation of 6.5706. Figure 8a and 8b show the linear prediction performance analysis of the ANFIS-PSO and ANFIS-GA. This proves that the ANFIS-PSO and ANFIS-GA can predict the experimental results of the cutting force with 91.9% and 93.98%, respectively, during the training process.

The ANFIS-PSO and ANFIS-GA approaches are shown in Figure 9a and Figure 9b for the second data group in the form of Test Data output. The MSE OF 38.43, RMSE OF 6.1992, and the ST.D. of 55.73 for the ANFIS-PSO, while the ANFIS-GA have a MSE of 14.1683, RMSE of 3.7641, and ST.D. of 3.4766. This analysis shows the accuracy of the ANFIS-PSO and ANFIS-GA prediction performance. From the analysis of the cutting force, the ANFIS-GA has the most accurate prediction, and the model measurement criteria and the actual and observed data processing are depicted in Figure 10a and Figure 10b, which were created to determine the coefficient of determination for the testing data group. The target and output values for the testing data are compared. To determine the coefficient of determination for the test data group was created, and the target, statistics R^2, output values of 90.1% and 92.1% for both the prediction method and test data for the cutting force were specified—standards for judging the outcomes.

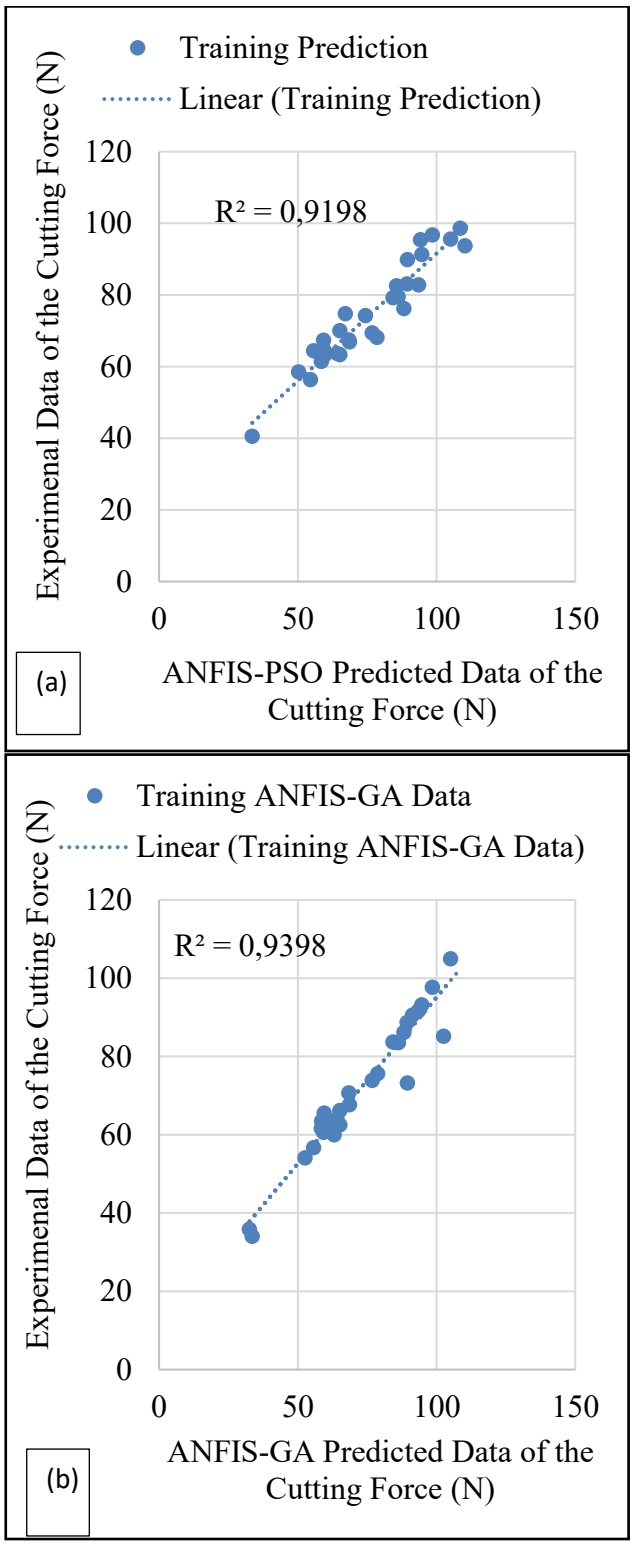

Figure-8. The comparative analysis of the Training R^2 predicted and experimental data for (a) ANFIS-PSO and (b) ANFIS-GA.

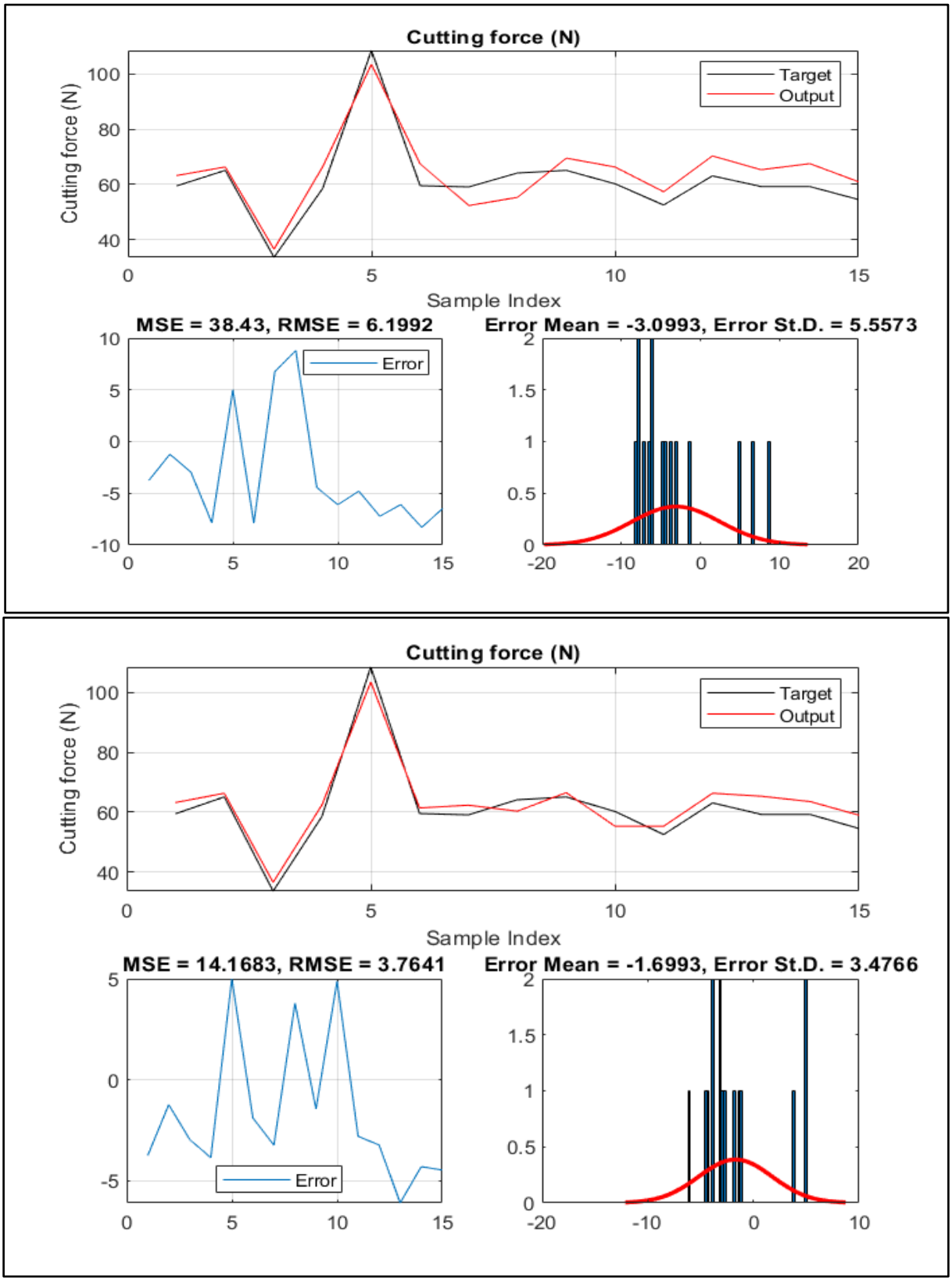

Figure-9. The comparative analysis of the testing data prediction with the experimental data for the (a) ANFIS-PSO and (b) the ANFIS-GA.

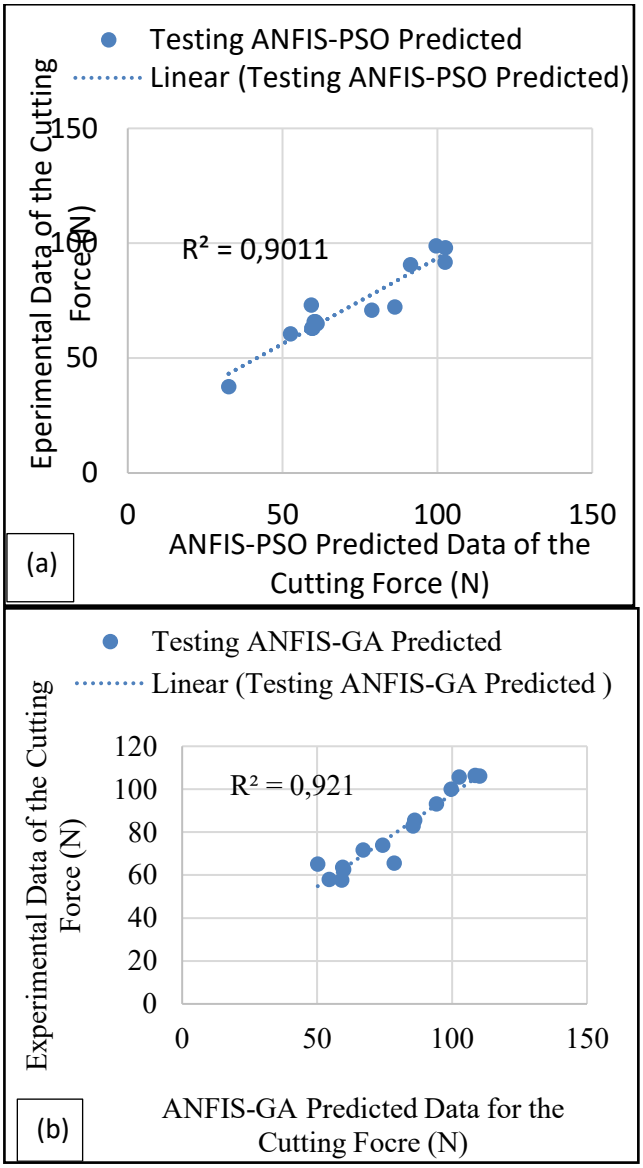

Figure-10. The comparative analysis of the testing R^2 predicted and experimental data for (a) ANFIS-PSO and (b) ANFIS-GA.

Statistical indicators showing the error were used to investigate the accuracy of the model generated in this study. The (13) to (17) Eqs. Introduce these indicators.

$$MSE = \frac{1}{50}\sum_{i=1}^{50}(Target_i - Output_i)^2 \quad (13)$$

$$RMSE = \sqrt{\frac{1}{50}\sum_{i=1}^{50}(Target_i - Output_i)^2} \quad (14)$$

$$MAE = \sqrt{\frac{1}{50}\sum_{i=1}^{50}|Target_i - Output_i|} \quad (15)$$

$$R^2 = \left(\frac{\sum(Target_i - \overline{Target})\,X\,(Output_i - \overline{Output})}{\sqrt{\sum(Target_i - \overline{Target})^2\,X\,\sum(Output_i - \overline{Output})^2}}\right)^2 \quad (16)$$

$$STD\ Error = \sqrt{\frac{1}{50}\sum_{i=1}^{50}(Target_i - Output_i)^2} \quad (17)$$

3.1 Study of Parameters on the Cutting Force via Surface Plot Analysis

Figure 11a shows the impact of cutting speed and feed rate on the cutting force, and the analysis was carried out at a constant machining length of 40 mm, machining depth of 2 mm, and helix angles of 30°. It shows that the cutting speed, when increased slightly, reduces the cutting force due to its ability to reduce the build-up edge at the cutting region [18]. However, as the feed rate increases, the cutting force increases because the feed rate increases vibration and can cause the cutting tool to wear faster, affecting the friction occurrences at the cutting region, which increases it [19]. This increase will also damage the workpiece surface finishing; the ability to predict and optimise this parameter greatly reduces cutting force. Also, Figure 11b depicts the surface plot analysis of the variable's parameter on the cutting force of Machining length vs. cutting speed. The machining length is another factor affecting cutting force. As the machining length increases, chip discontinuity affects the workpiece's surface and the cutting process. Cutting fluid is needed to remove the discontinuous chips from the cutting region [20]. Most of the time, when the machining length is too long at the centre of the workpiece, the occurrences of high vibration are normal, and at that time, there is a tendency for the cutting tool to fail due to wear experimentally.

Figure 11c shows the relationship between the machining length and feed rate. From the illustration of the graph, the colour variation shows that both parameters increase the cutting force as the colour changes from deep blue to light blue, and the final changes to yellow to increase the machining length and feed rate in this study. The cutting speed is 3000 rpm, the machining depth is 2 mm, and the helix angle is 30°. Figure 11d also shows that the trend of the cutting force decreases as the machining depth decreases with the machining length. The feed rate, helix angle, and cutting speed are kept at 200 mm, 30°, and 3000 rpm [21]. The surface plot analysis of the variable's parameter on the cutting force of Helix angle vs. Machining length is given in Figure 11e. This means that the helix angle tends to increase the cutting force because as the machining length increases with the angle of cut, which is the helix angle, the chips increase, and at that time, the weight and the discontinuous chips add up to the cutting force. Because the relative movement is part of what determines the cutting force, the weight of the chips

at the cutting region, and the vibration that occurs. The surface plot shows that the cutting speed and the helix angle have little relationship because both parameters function parallelly [22-23]. That means the cutting speed tends to reduce the cutting force, so the helix angle increases the cutting force.

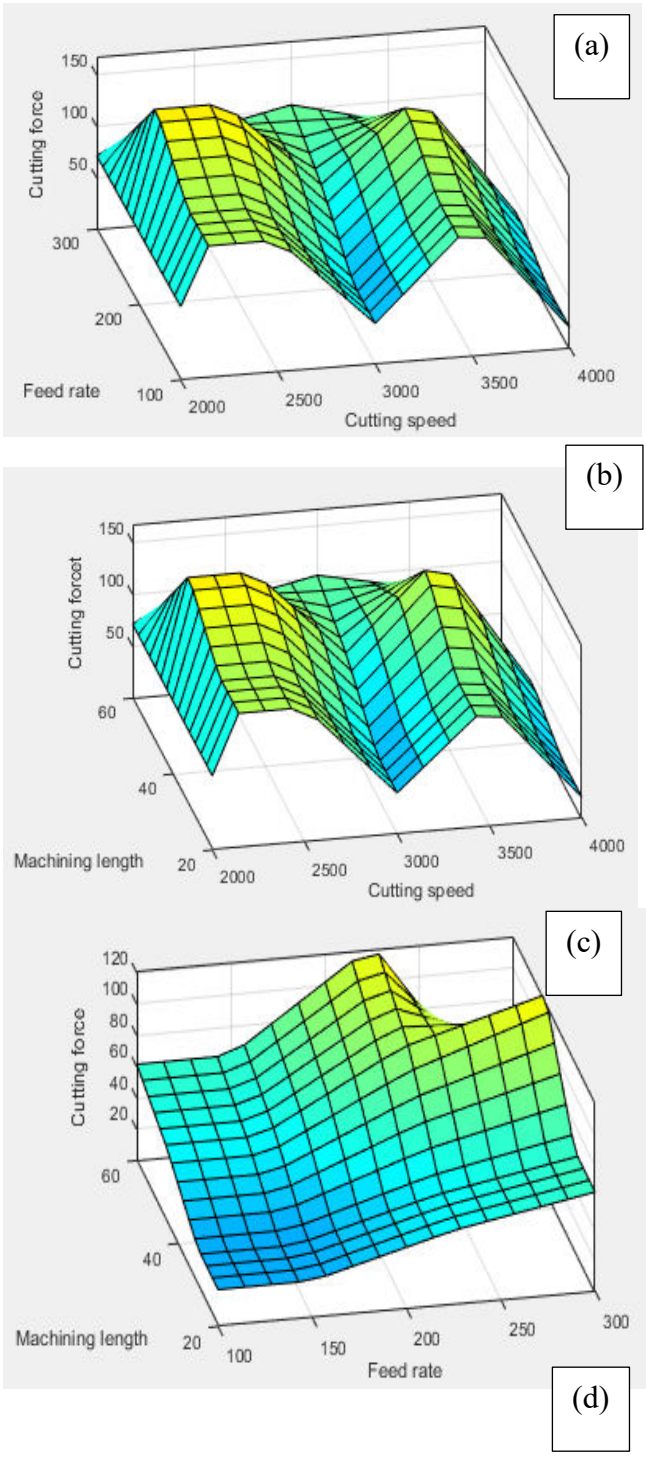

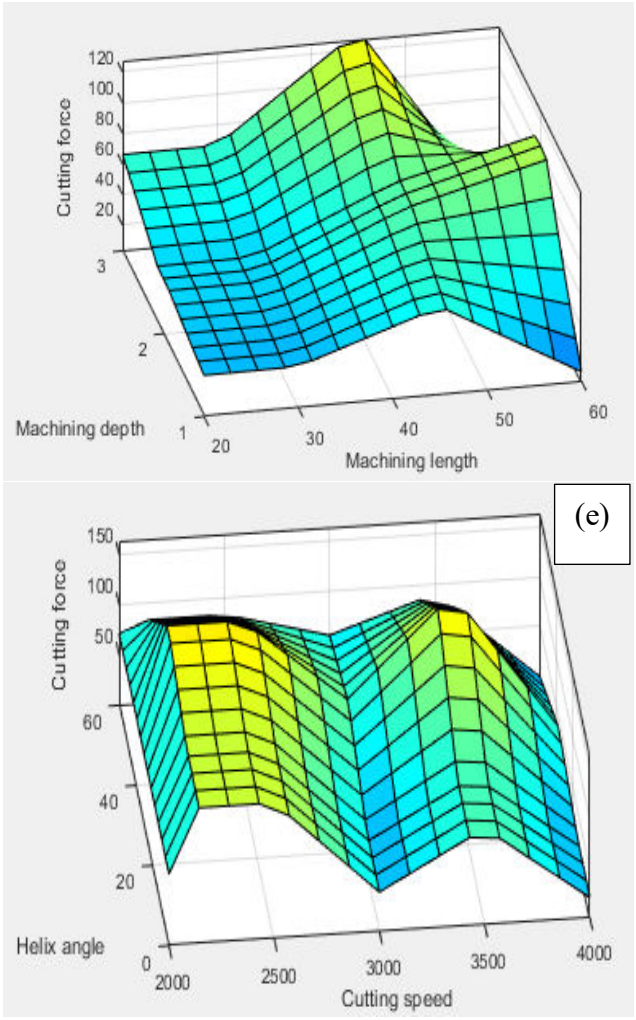

Figure-11. The surface plot analysis of the variable's parameter on the cutting force (a) Cutting speed vs Feed rate, (b) Machining length vs cutting speed, (c) Feed rate vs Machining length, (d) Machining length vs Machining and (e) Cutting speed vs Helix angle.

4. CONCLUSIONS

This cutting force analysis project was carried out during the machining of Al-8112 alloys via ANFIS-PSO. The show considered five (5) major cutting parameters, such as cutting speed, feed rate, machining length, helix angle, and machining depth, varies in five (5) concentration levels under TiO_2 nano-lubricant cutting conditions. The dynamometer was employed during the experiment to determine the cutting force from the three (3) axes, and the average value was obtained. The ANFIS-PSO was employed to train a model via MATLAB software, and the model was tested with some experimental values. The ratio of training and testing is 35:15. Therefore, the study has the following conclusions:

i. It shows from the prediction that ANFIS-PSO was able to predict the cutting with five (5) factors and

five (5) levels having a coefficient of determination R^2 as 91.98% for training data and 90.11% for the testing data when compared with the experimental data. Also, the ANFIS-GA predicted the cutting force with 93.98% for the training data and for the testing data 92.1%.

ii. The mean absolute percentage error (MAPE) is also one way of determining the accuracy of the prediction analysis. The ANFIS-PSO has an 8.7607 compared with the ANFIS-GA of 5.9482. The smaller the MAPE, the better the prediction accuracy of the model.

iii. The study shows that the interaction of the surface plot of the cutting parameters shows a good relationship with the helix angle and the machining length.

This study will recommend further study of hybridisers' application of the hybrid nano lubricant and the optimisation of the interaction between heuristic and metaheuristic techniques in predicting the cutting force.

REFERENCES

[1] Gupta, M. K., Korkmaz, M. E., Sarıkaya, M., Krolczyk, G. M., Günay, M., and Wojciechowski, S. 2022. Cutting forces and temperature measurements in cryogenic assisted turning of AA2024-T351 alloy: An experimentally validated simulation approach. Measurement, 188, 110594. https://doi.org/10.1016/j.measurement.2021.110594.

[2] Aydın, M., and Köklü, U. 2024. Analysis of cutting forces at different spindle speeds with straight and helical-flute tools for conventional-speed milling incorporating the effect of tool runout. Mechanics Based Design of Structures and Machines, 52(2), 867-893. https://doi.org/10.1080/15397734.2022.2125878.

[3] Okokpujie, I. P., and Tartibu, L. K. 2023. Cutting Fluid and Its Application with Different Delivering Machining Techniques. In Modern Optimization Techniques for Advanced Machining: Heuristic and Metaheuristic Techniques (pp. 25-39). Cham: Springer Nature Switzerland.https://doi.org/10.1007/978-3-031-35455-7_2

[4] Okokpujie, I. P., Tartibu, L. K., Sinebe, J. E., Adeoye, A. O., and Akinlabi, E. T. 2022. Comparative study of rheological effects of vegetable oil-lubricant, TiO2, MWCNTs nano-lubricants, and machining parameters' influence on cutting force for sustainable metal cutting process. Lubricants, 10(4), 54. https://doi.org/10.3390/lubricants10040054

[5] Jain, V., and Raj, T. 2018. Prediction of cutting force by using ANFIS. International Journal of System Assurance Engineering and Management, 9, 1137-1146. https://doi.org/10.1007/s13198-018-0717-x

[6] Okokpujie, I. P., and Tartibu, L. K. 2023. Cutting Force Optimisation Under ANN and QRCCD. In Modern Optimization Techniques for Advanced Machining: Heuristic and Metaheuristic Techniques (pp. 201-231). Cham: Springer Nature Switzerland. https://doi.org/10.1007/978-3-031-35455-7_10.

[7] Surajudeen-Bakinde, N. T., Faruk, N., Popoola, S. I., Salman, M. A., Oloyede, A. A., Olawoyin, L. A., and Calafate, C. T. 2018. Path loss predictions for multi-transmitter radio propagation in VHF bands using Adaptive Neuro-Fuzzy Inference System. Engineering Science and Technology, an International Journal, 21(4), 679-691. https://doi.org/10.1016/j.jestch.2018.05.013.

[8] Okokpujie, I. P., and Tartibu, L. K. 2023. Adaptive Neuro-Fuzzy Inference System for Prediction of Surface Roughness Under Biodegradable Nano-lubricant. In Modern Optimization Techniques for Advanced Machining: Heuristic and Metaheuristic Techniques (pp. 289-311). Cham: Springer Nature Switzerland. https://doi.org/10.1007/978-3-031-35455-7_13.

[9] Alarifi, I. M., Nguyen, H. M., Naderi Bakhtiyari, A., and Asadi, A. 2019. Feasibility of ANFIS-PSO and ANFIS-GA models in predicting thermophysical properties of Al2O3-MWCNT/oil hybrid nanofluid. Materials, 12(21), 3628. https://doi.org/10.3390/ma12213628.

[10] Zand, J. P., Katebi, J., and Yaghmaei-Sabegh, S. 2024. A hybrid clustering-based type-2 adaptive neuro-fuzzy forecasting model for smart control systems. Expert Systems with Applications, 239, 122445. https://doi.org/10.1016/j.eswa.2023.122445.

[11] Zhang, H., Sun, B., and Peng, W. 2024. A novel hybrid deep fuzzy model based on gradient descent algorithm with application to time series

forecasting. Expert Systems with Applications, 238, 121988. https://doi.org/10.1016/j.eswa.2023.121988.

[12] Sowmya, R., Premkumar, M., and Jangir, P. 2024. Newton-Raphson-based optimiser: A new population-based metaheuristic algorithm for continuous optimisation problems. Engineering Applications of Artificial Intelligence, 128, 107532. https://doi.org/10.1016/j.engappai.2023.107532.

[13] Okokpujie, I. P., and Tartibu, L. K. 2023. Global Machining Prediction and Optimisation. In Modern Optimization Techniques for Advanced Machining: Heuristic and Metaheuristic Techniques (pp. 61-90). Cham: Springer Nature Switzerland. https://doi.org/10.1007/978-3-031-35455-7_4.

[14] Chaudhari, S., Thakare, A., and Anter, A. M. 2024. PSOGSA: A parallel implementation model for data clustering using new hybrid swarm intelligence and improved machine learning technique. Sustainable Computing: Informatics and Systems, 41, 100953. https://doi.org/10.1016/j.suscom.2023.100953.

[15] Mottahedi, A., Sereshki, F., and Ataei, M. 2018. Overbreak prediction in underground excavations using hybrid ANFIS-PSO model. Tunnelling and Underground Space Technology, 80, 1-9. https://doi.org/10.1016/j.tust.2018.05.023

[16] Qasem, S. N., Ebtehaj, I., and Riahi Madavar, H. 2017. Optimising ANFIS for sediment transport in open channels using different evolutionary algorithms. Journal of Applied Research in Water and Wastewater, 4(1), 290-298.

[17] Marrel, A., and Iooss, B. 2024. Probabilistic surrogate modeling by Gaussian process: A review on recent insights in estimation and validation. Reliability Engineering & System Safety, 110094. https://doi.org/10.1016/j.ress.2024.110120.

[18] Assurin, S. R., Mativenga, P., Cooke, K., Sun, H., Field, S., Walker, M., ... and Mortensgaard, M. F. 2024. Establishing cutting conditions for dry drilling of aluminium alloy stack materials. Proceedings of the Institution of Mechanical Engineers, Part B: Journal of Engineering Manufacture, 238(1-2), 214-222. https://doi.org/10.1177/09544054221147712

[19] Korkmaz, M. E., Gupta, M. K., Çelik, E., Ross, N. S., and Günay, M. 2024. A sustainable cooling/lubrication method focusing on energy consumption and other machining characteristics in high-speed turning of aluminum alloy. Sustainable Materials and Technologies, 40, e00919. https://doi.org/10.1016/j.susmat.2024.e00919

[20] Okokpujie, I. P., Sinebe, J. E., and Tartibu, L. K. 2024. Study of the Effects of Five Different Machining Fluids on the Surface Hardness and Corrosion Behaviour of Al6061 Alloy. Journal of Advanced Research in Applied Sciences and Engineering Technology, 42(2), 72-88. https://doi.org/10.37934/araset.42.2.7288.

[21] Kuo, C., Chen, C., Jiang, S., and Chen, Y. 2023. Effects of the tool geometry, cutting and ultrasonic vibration parameters on the cutting forces, tool wear, machined surface integrity and subsurface damages in routing of glass-fibre-reinforced honeycomb cores. Journal of Manufacturing Processes, 104, 59-75. https://doi.org/10.1016/j.jmapro.2023.08.051.

[22] Okokpujie, I. P., and Tartibu, L. K. 2021. Experimental analysis of cutting force during machining difficult to cut materials under dry, mineral oil, and TiO2 nano-lubricant. Journal of Measurements in Engineering, 9(4), 218-230. https://doi.org/10.21595/jme.2021.22186.

[23] Yang, K., Pan, J., Cao, Z., and Zhu, Y. 2024. Investigation of the Effect Mechanism of Cutting Sequence on Spiral Milling of CFRP/Ti Laminates Under Ultrasonic-Assisted Conditions. International Journal of Precision Engineering and Manufacturing, 1-19. https://doi.org/10.1007/s12541-0.